JOURNAL OF SPACECRAFT AND ROCKETS
Vol. 30, No. 2, March-April 1993

Numerical Study of the Flow Establishment Time in Hypersonic Shock Tunnels

J. Y. Lee* and M. J. Lewis†
University of Maryland, College Park, Maryland 20742

A numerical study of unsteady hypersonic viscous flows in two-dimensional hypersonic shock tunnels is presented. The numerical experiments on the combined nozzle/model flows, using the configurations mounted in the test section of a 14.7 ft long shock tunnel, which has a design Mach number of M_e=6 and the stagnation temperature of T_0=3,063°R, have been performed by solving the two-dimensional Navier-Stokes equations with an upwind total variation diminishing scheme in the alternating direction implicit form. The flow establishment times around aerodynamic models, such as a flat plate, a biconvex airfoil, thin and thick double wedges, and a circular cylinder, are calculated and compared. As a result, the present analysis shows that, for the most severely separated case of a circular cylinder, the flow becomes stabilized within about 8 ms, including the starting process, and its nondimensional flow establishment time, $(\tau_p U_\infty)/L$ is 46. The flow establishment time increases.

Nomenclature

C_p = pressure coefficient
D = diameter of the circular cylinder, 0.534 ft
e_t = total energy
L = characteristic length (D for a circular cylinder)
M = Mach number
p = static pressure, atm
R_e = Reynolds number, $\rho_\infty l a_\infty/\mu_\infty$
T = static temperature, °R
t = time, s
t/c = thickness ratio of model
u,v = x and y velocity components in Cartesian coordinates
γ = ratio of specific heats
ρ = density
τ = flow establishment time, s

Subscripts

e = nozzle exit condition
o = reservoir condition
w = condition at wall
p = pressure
Q = heat transfer
$*$ = nozzle throat condition
∞ = freestream condition in test section

Introduction

RENEWED interest in hypersonic research, due to such projects as the National Aero-Space Plane (NASP)[1] and the Aeroassist Flight Experiment (AFE),[2] has re-emphasized the need for state-of-the-art test facilities in the hypersonic flight regime. Because of the extreme of temperatures and pressures associated with hypersonic flow, duplication of the flight environment in the laboratory is extremely difficult, and various test schemes to simulate more realistic hypersonic flow have been developed with varying degrees of success.[3,4]

Aerodynamic simulation is primarily dependent on matching Mach number between flight test and experiment. Mach numbers up to eight are relatively easy to produce in continuous wind tunnels. However, it is difficult to use air as the test medium because a reservoir temperature must be provided that is high enough to avoid liquefaction of the air as it expands through the nozzle. For example, a reservoir temperature of about 2000°R is near the practical limit for all continuous wind tunnels because of the difficulty of providing adequate thermal protection for the high temperature components of the facility. Therefore, higher Mach number facilities rely on thermal inertia and short duration runs to address the thermal protection problem. In particular, impulse facilities can be used to simulate high Mach numbers with high enthalpy and high Reynolds number, albeit with very short test times.

The time required to establish steady flow in complex regions with viscous interaction and flow separation remains an important question in impulse facilities with short run times such as shock tubes, shock tunnels, and piston- and arc-driven facilities. Measurements in shock tubes and shock tunnels at Calspan[5] have indicated the separated regions can take from 100 μs to several milliseconds to become fully established. Therefore, there is always a question as to whether or not the test times are sufficient to allow the establishment of certain types of steady flows over aerodynamic models, especially flows involving strong viscous effects such as boundary-layer growth and separated flow. If available test times are not long enough to obtain a steady-state flow over aerodynamic models, the experimental data from these facilities are not reliable for accurately representing the simulated flowfields. To design experiments in impulsive facilities properly and to interpret data from such facilities, it is useful to understand how the flow approaches the steady-state condition by knowing the transient flowfield and the flow establishment time around a given model.

The experimental studies by Smith[6] and Amann[7] showed that the flowfield contained in the starting process in a hypersonic shock tunnel consists of a primary shock, a secondary shock, an interface resulting from Mach reflections, and boundaries of a separated mass of gas. In addition, the flowfield with an aerodynamic model/shock tunnel will become more complicated, including interactions between attached or detached shocks on a stagnation region of model and the boundary layer on the nozzle wall and strong separation on a rear stagnation region of models.

Important advances have been made in computational fluid dynamics (CFD) applied to hypersonic aerodynamics during the past several years. Hypersonics is also an excellent proving ground for CFD and a likely area for complementary roles with wind tunnels. Since the computer is not burdened by high pressure and temperature operational problems as in the ground test facilities, the extremes of Mach number and Reynolds number can be explored.

Presented as Paper 91-1706 at the AIAA 22nd Fluid Dynamics, Plasmadynamics, and Lasers Conference, Honolulu, HI, June 24–27, 1991; received Feb. 20, 1992; revision received July 20, 1992; accepted for publication Sept. 8, 1992.

*Research Assistant, Department of Aerospace Engineering. Student Member AIAA.

†Assistant Professor, Department of Aerospace Engineering. Member AIAA.

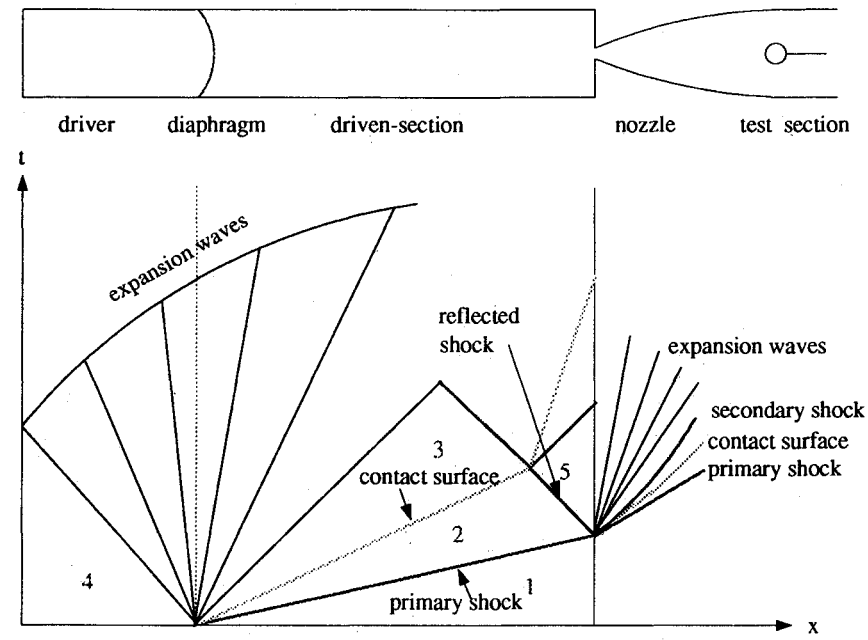

Fig. 1 Shock tunnel and *x-t* diagram.

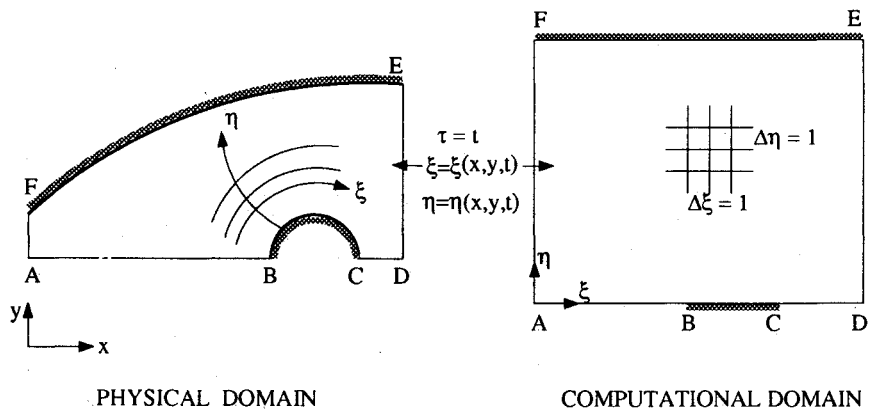

Fig. 2 Generalized curvilinear coordinate transformation.

Previous work by Byun, et al.[8] calculated the flow establishment time over a circular cylinder using the time-dependent alternating direction implicit (ADI) type total variation diminishing (TVD) code that solves the thin-layer Navier Stokes equations. For a circular cylinder in the M_e=6 designed 15 ft long nozzle, it was shown that flow establishment takes about 9.5 ms, including the starting process. But the prediction of a strong separation region using the thin-layer approximation was of questionable accuracy. In high Reynolds number viscous flows, the effects of viscosity are concentrated near solid boundaries and in wake regions. For most aerodynamic problems where the flow separation is moderate, the predictions of the thin-layer Navier-Stokes equations show excellent agreement compared with experiment data. However, the thin-layer approximation can break down for low Reynolds numbers and in regions of massive flow separation. Because the flow establishment time strongly depends on the viscous interaction and flow separation within the boundary layer, the thin-layer approximation may not be appropriate for this study on the flow establishment time.

In the present work, the computer program TIMETVD, originally developed by Yee and Harten[9] and Yee[10] at the NASA Ames Research Center, which solves the two-dimensional thin-layer Navier-Stokes equations, has been modified to solve the full Navier-Stokes equations. The numerical experiments on the combined nozzle/model flows, using the various configurations mounted in the test section, such as a flat plate, a biconvex airfoil, thin and thick double wedges, and a circular cylinder, will be presented. The flow establishment time over the aforementioned models will be calculated and compared for the relative effects of geometry on the flow process.

Hypersonic Shock Tunnel

Shock tunnels[3] typically include a shock tube, a nozzle attached to the end of the driven section of the shock tube, and a diaphragm between the nozzle and the driven tube, as shown in Fig. 1. A diaphragm between a driver and a driven gas in the shock tube is ruptured and the high-pressure driver gas rushes into the driven section, setting up a shock wave that compresses and heats the driven gas. When the generated shock reaches the end of the driven tube, the diaphragm at the nozzle entrance is ruptured. The shock is reflected from the end of the driven tube, and a constant property region with the heated and compressed gas behind the reflected shock is generated for a very short time. This region is represented by region 5 in Fig. 1. The flow in region 5 is at rest, even though the reflected shock moves. Since the flow in region 5 has gone through two shock waves, enthalpy and pressure are both quite high, its enthalpy usually being more than twice the static enthalpy of the flow in region 2. This very high temperature and pressure gas expands through the convergent-divergent nozzle to deliver high Mach number flow at the test section. In essence, region 5

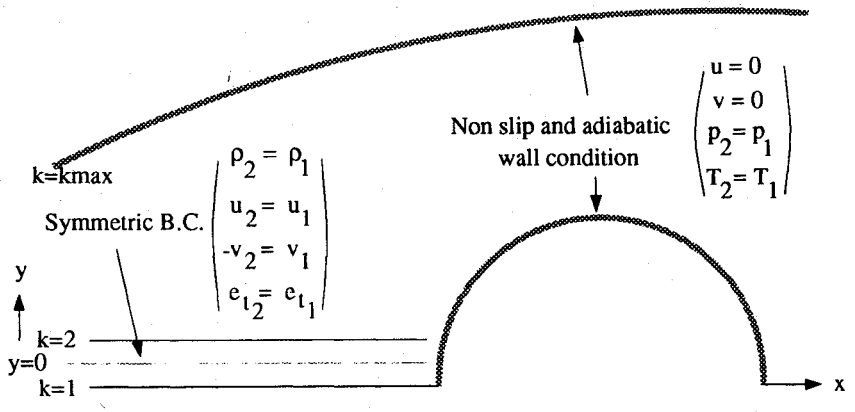

Fig. 3 Boundary conditions at the surface and the centerline.

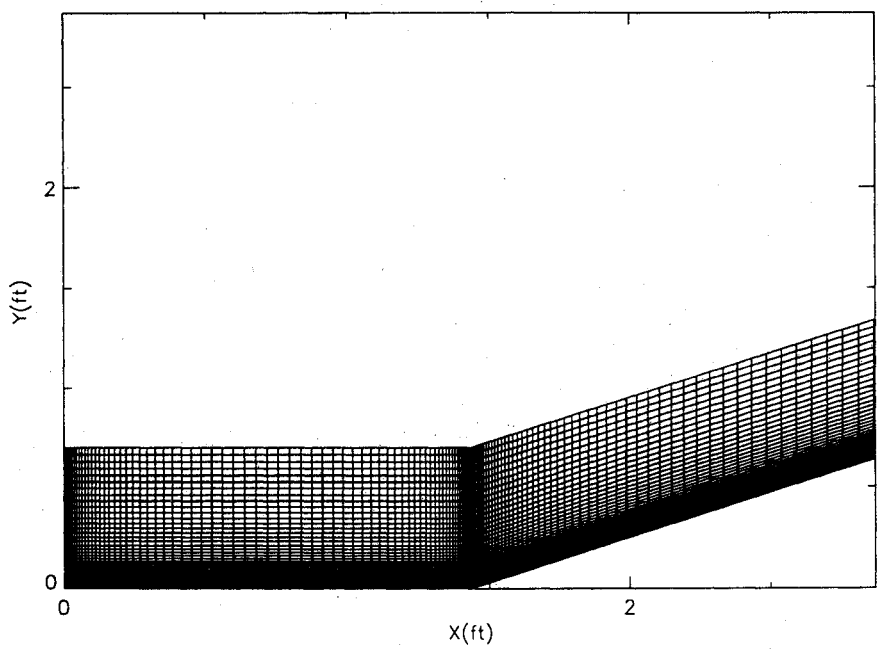

Fig. 4 H-type (121×61) grid for 24-deg compression corner flow.

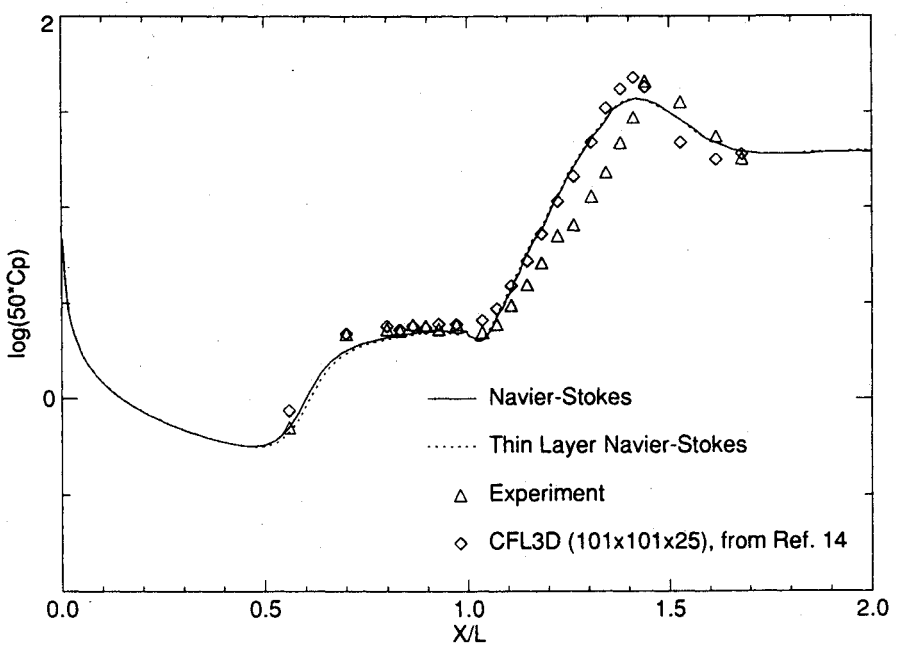

Fig. 5 Comparison of computed and experimental surface pressure for 24-deg compression corner.

functions as the settling chamber of the wind tunnel. The flow duration in the shock tunnel is typically less than 10 ms.[4,11] Therefore the wall temperature does not reach the critical melting point, and there is no temperature limit, as there is in the conventional blowdown hypersonic wind tunnel. The pressure in region 5 is typically on the order of 1000 atm. Hence, the shock tunnel produces a very high Mach number (in excess of 15) and a Reynolds number on the order of 10^7 with proper enthalpy.

Numerical Algorithm

The TIMETVD code that solves the two-dimensional Navier-Stokes equations in the generalized curvilinear coordinates as shown in Fig. 2 is used for the present study. The numerical algorithm used is the TVD scheme in the ADI form developed by Yee and Harten[9] and Yee,[10] which gives second-order accuracy in space and time. Perfect gas and laminar flow is assumed, and the inviscid components of flux are described with Roe's[12] averaging and Harten's entropy fix with Yee's second-order corrections. The explicit viscous terms are discretized using central differences. For the present study, the implicit and explicit viscous terms in the streamwise and cross direction are restored for full Navier-Stokes solutions.

Boundary Conditions

At the nozzle wall and the surface of the models, the no-slip condition is satisfied for the viscous flow and the pressure on the surface is obtained from the normal momentum equation. For temperature, the adiabatic wall condition is applied to the surface.

At the centerline of the nozzle, the symmetric boundary conditions are applied. Therefore, the grid system is selected such that grid lines $k=1$ and 2 are symmetrical with respect to the body axis, $y=0$, as shown in Fig. 3.

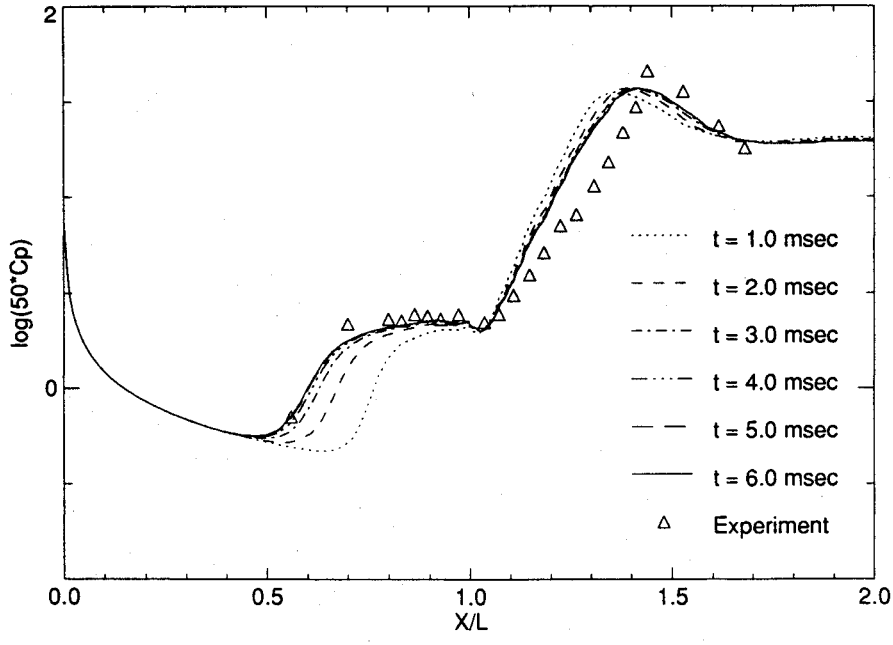

Fig. 6 Time history of surface pressure for 24-deg compression corner.

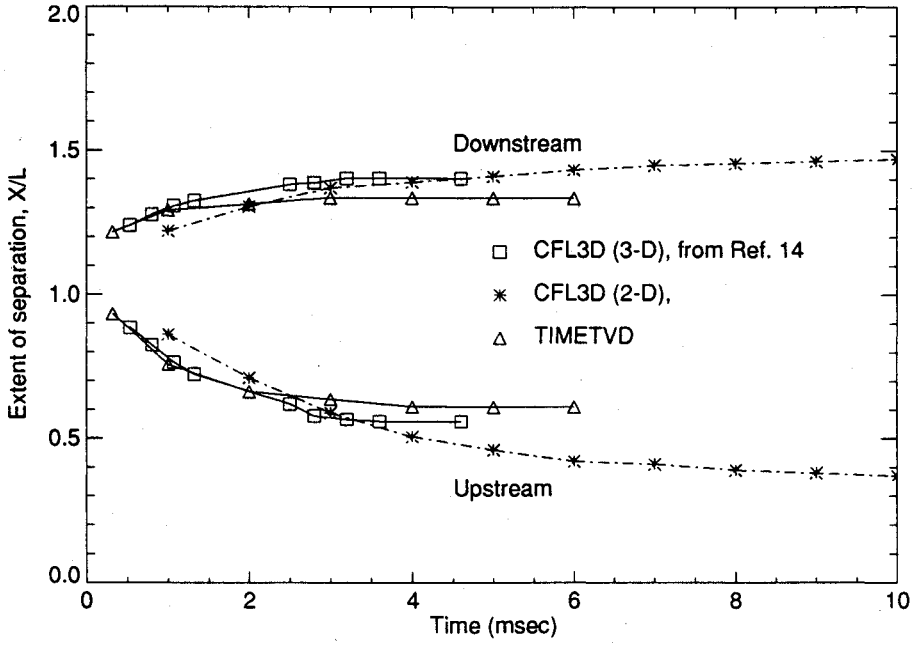

Fig. 7 Time history of separation extent for 24-deg compression corner.

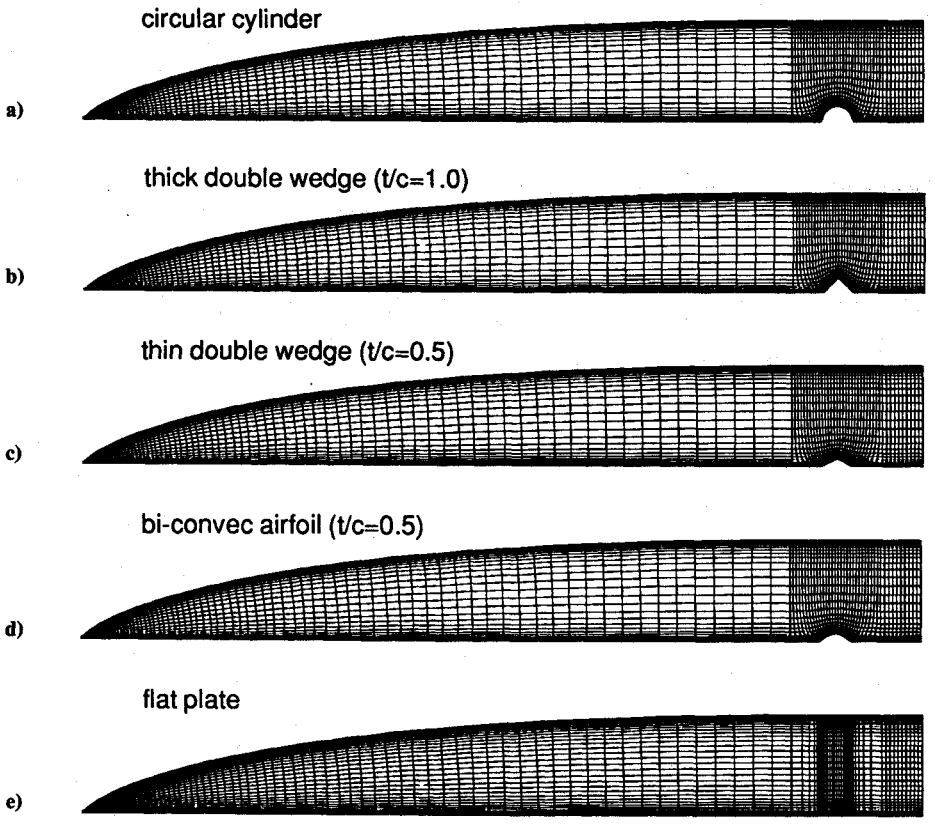

Fig. 8 H-type (181×40) grids on aerodynamic models in a shock tunnel.

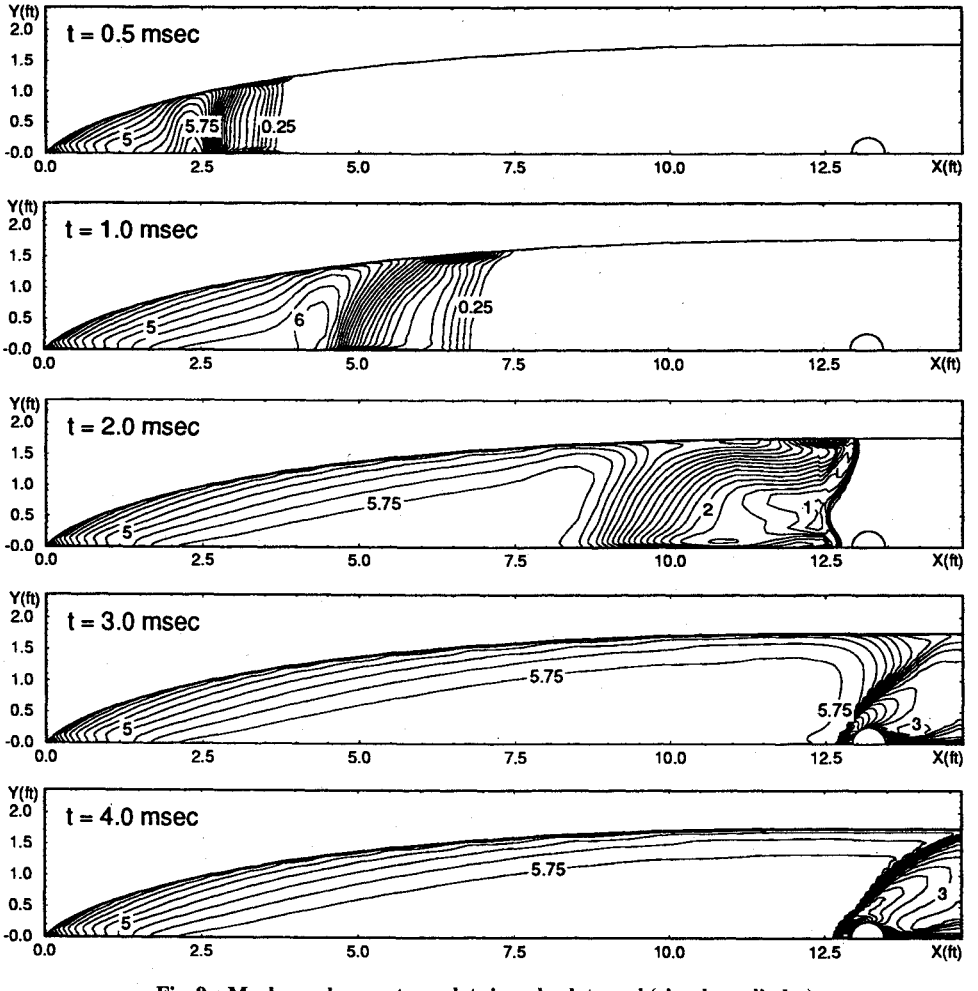

Fig. 9 Mach number contour plots in a shock tunnel (circular cylinder).

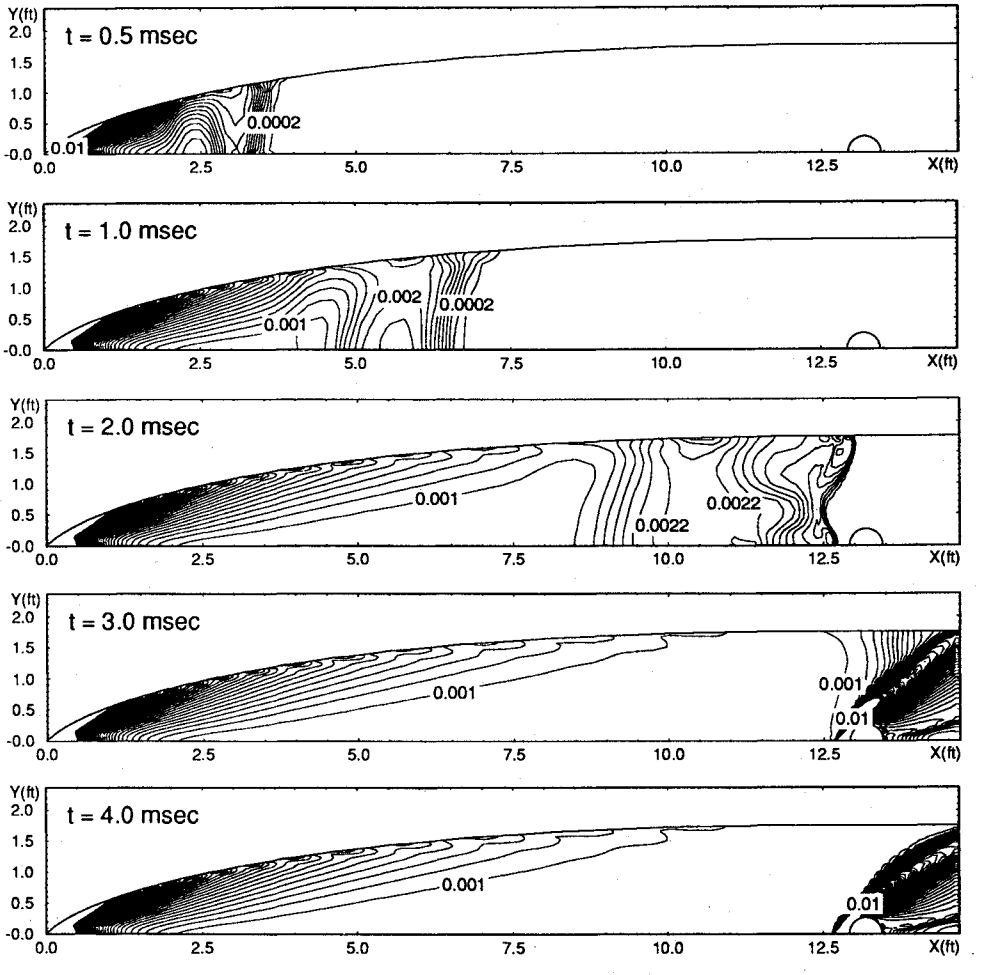

Fig. 10 Pressure contour plots in a shock tunnel (circular cylinder).

For supersonic inflow boundaries, all flow variables are specified. In the case of supersonic outflow, all variables are extrapolated from the adjacent point.

Numerical Results and Discussion

For the purpose of code validation, the two-dimensional flow over a compression corner that is formed by the interaction of a flat plate and a 24-deg wedge is calculated and compared with results from the Calspan 48-in. shock tunnel. Rudy et al.[14] used this compression corner to validate the four Navier-Stokes codes, such as CFL3D, USA-PG2, NASCRIN, and LAURA. The computation of the TIMETVD code is also compared with the results of other Navier-Stokes codes.

For the calculation of the flow establishment times over aerodynamic models, a two-dimensional shock tunnel that has a 14.7 ft long nozzle, with a contour generated by the method of characteristics to reach the design Mach number, M_e=6, at the exit, is used. The flow establishment times around aerodynamic models, such as a flat plate, a biconvex airfoil, thin and thick double wedges, and a circular cylinder, are calculated.

Code Validation

The 121×61 grid of the compression corner is shown in Fig. 4. The nominal flow conditions are M_∞=14.1, T_∞=160°R, and R_e =7.2×10^4 (1/ft). The wall temperature T_w is 535°R. The Reynolds number is low enough that the flow remains completely laminar, thereby eliminating the issue of turbulence modeling. Furthermore, even though the freestream Mach number is high, the freestream temperature is low enough that there are no significant chemical reaction effects.

Figure 5 shows the comparison of the computed surface pressure coefficient with experimental data and the CFL3D computation, where comparison shows excellent agreement with the experimental data in the region of separation but overpredicted on the surface of the wedge. Compared with the prediction of CFL3D, the present results of the TIMETVD code give good accuracy in the calculation of the surface pressure.

Figure 6 shows the time history of surface pressure, where it can be seen that the separated region propagating toward the upstream and the unsteady separated flow reaches a steady state in about 5 ms.

Figure 7 shows the positions of the upstream and downstream boundaries of the separated flow region as functions of time. The computation of the TIMETVD code shows that, to reach its steady state, the separated flow of the upstream region requires about 4 ms and at the downstream about 3 ms. The flow in the experiment reached a steady state in approximately 4 ms, and total run time was about 10 ms. Compared with the two-dimensional computation of CFL3D, the result of the TIMETVD code is close to the result of the three-dimensional calculation of CFL3D, which shows better accuracy.

Therefore, through the validation study discussed earlier, it is concluded that the TIMETVD code is capable of accurately representing both qualitatively and quantitatively the complex hypersonic flow with strong viscous-inviscid interaction considered.

Analysis of the Flow Establishment Time

The time required to establish steady flow over an aerodynamic model having complex regions of viscous interaction and flow separation becomes a very important issue in hypersonic impulse

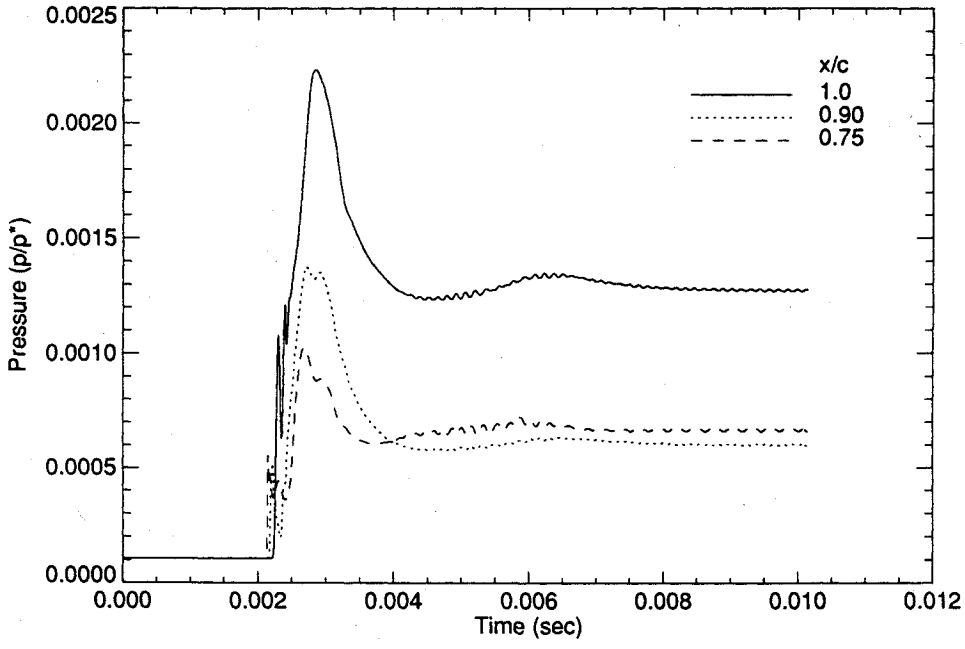

Fig. 11 Pressure distributions in the separated region of a circular cylinder.

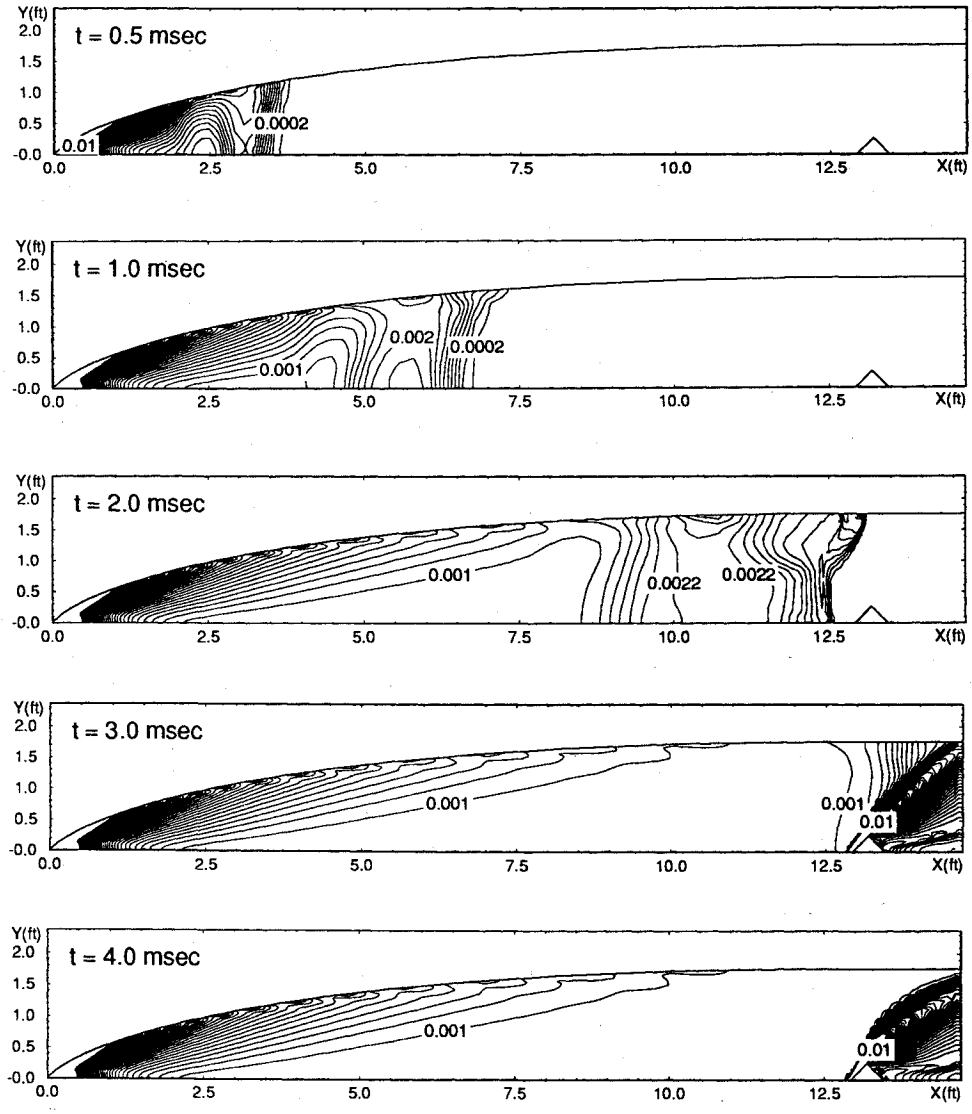

Fig. 12 Pressure contour plots in a shock tunnel (thick double wedge).

facilities with short testing times. Holden[5] expressed the characteristic establishment time τ_{est} for a given configuration in the form

$$\frac{\tau_{est} U_\infty}{L} = T(M_e, R_{eL}, T_w/T_o)$$

where the flow establishment time τ_{est} is defined when the pressure or heat transfer reaches 98% of its final steady values. The characteristic velocity U_∞ is the freestream velocity, and L is a characteristic dimension related to the length of the interaction region through the parameter T. From experiments, Holden observed that the nondimensional establishment time is weakly influenced by the Mach number and Reynolds number of the freestream. The establishment time is directly proportional to the scale of the separated region and decreases with increasing freestream velocity. Through correlations of the measurements in the base region of a sphere, Holden showed that just under 30 body lengths of flow ($\tau_p U_\infty/D=27.9$) were required for the pressure in a base region to stabilize and that the heat transfer to this region took a factor of two longer ($\tau_Q U_\infty/D=70$) to reach equilibrium.

In this study, the flow establishment time over a model in a hypersonic shock tunnel is calculated by solving the entire flowfield inside the nozzle, which includes an aerodynamic model. Therefore, the results of numerical simulation will include time for the starting process and time for the flow establishment over the model as the actual shock tunnel experiment proceeds.

The contours of a two-dimensional shock tunnel were generated by the method of characteristics to obtain the design Mach number, $M_e=6$, at the test section. The shock tunnel nozzle has a throat height of 0.066 ft, an exit height of 3.49 ft, and a length of 14.7 ft. The model is located at 12.9 ft measured from the throat, and its chord length is set to 0.534 ft.

Figure 8 shows the H-type (181×40) grids on the aerodynamic models used in the computational hypersonic shock tunnel nozzle. Aerodynamic models installed in the test section are a circular cylinder, thin and thick double wedges ($t/c=0.5$ and 1.0), a biconvex airfoil ($t/c=0.5$), and a flat plate.

The stagnation pressure P_o in Region 5 of the shock tunnel diagram shown in Fig. 1 is set to 1215 atm, and the stagnation temperature T_o to 3063°R. To start the shock tunnel, the initial pressure and temperature in the nozzle are set to 0.07 atm and 520°R. The freestream velocity U_∞ in the test section is 4960 ft/s, and the unit Reynolds number R_e at the exit is 4.4×10^7 (1/ft).

The flow establishment time will be determined as the time required for flow to reach 98% of the steady value of pressure minus the time for the secondary shock to pass the assumed location of the numerical sensor. The pressure and temperature are calculated from the surface at $x/c=0.75$, 0.90, and 1.0.

Flow over a Circular Cylinder

Mach number and pressure contours over a circular cylinder in the hypersonic shock tunnel at time t =0.5, 1.0, 2.0, 3.0, and 4.0 ms are presented in Figs. 9 and 10, respectively. Notice that, at t =0.5 and 1.0 ms, there is a starting shock structure, which consists of the primary and secondary shock and an interface resulting from Mach reflection as indicated from Amann's experiment.[7] After the starting shock passes the circular cylinder, the detached bow shock in front of the stagnation region and the separated boundary-layer flow begin to stabilize. From the surface pressure record at the rear stagnation point, $x/c=1.0$, in Fig. 11, note that the secondary shock passes at time t =3.0 ms, and that the unsteady separated boundary-layer flow becomes stabilized at about t =8.0 ms. Therefore, the longest flow establishment time for pressure τ_p is about 5.0 ms.

Flow over a Thick Double Wedge

For a thick ($t/c=1.0$) double wedge, Fig. 12 shows pressure contours with a starting shock and the transient oscillation of a detached bow shock. Figure 13 shows a close-up of velocity vectors at t =7.7 ms, where a detached shock is formed in front of the thick double wedge because of its large wedge angle (45 deg). At the rear region of the double wedge the boundary layer becomes severely separated. Figure 14 shows the pressure record on the surface at $x/c=1.0$; the secondary shock passes at $t=3.0$ ms and the flow becomes stabilized at about $t=6.0$ ms. Therefore, the longest flow establishment time for pressure τ_p is estimated to be about 3.0 ms.

Flow over a Thin Double Wedge

For a thin ($t/c=0.5$) double wedge, Fig. 15 shows a close view of the test section at $t=6.1$ ms, where it can be seen that an attached oblique shock is formed at the leading edge of the thin double wedge, and the flow behind the shock is deflected. From the pressure records on the surface at $x/c=0.75$ in Fig. 16, the flow becomes stabilized at time $t=4.5$ ms. Therefore, the longest flow establishment time τ_p is determined to be 1.5 ms.

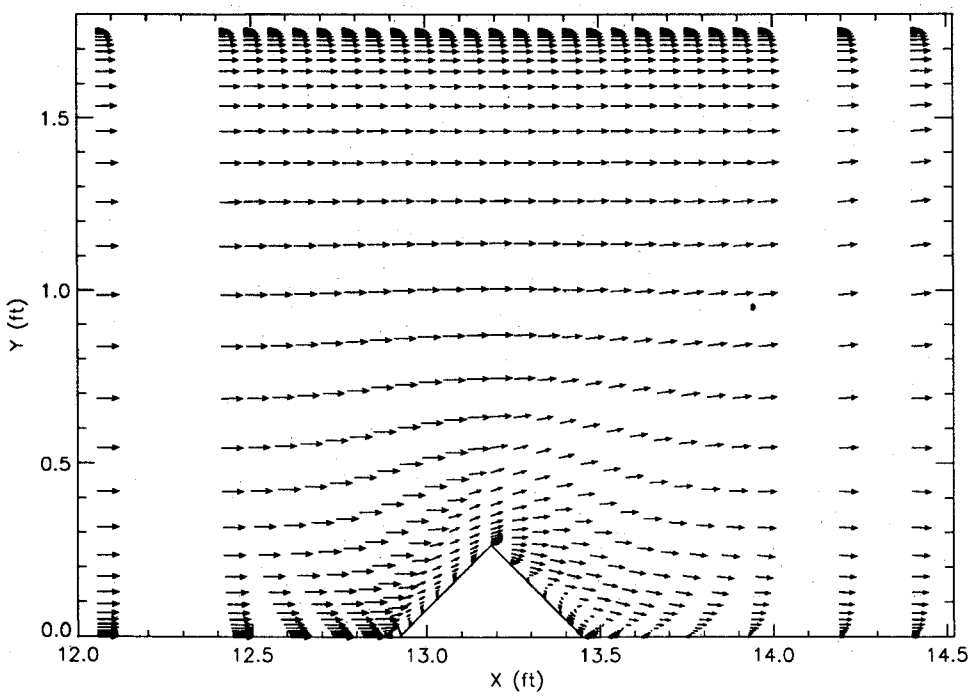

Fig. 13 Close-up of velocity vectors on a thick double wedge at t =7.7 ms.

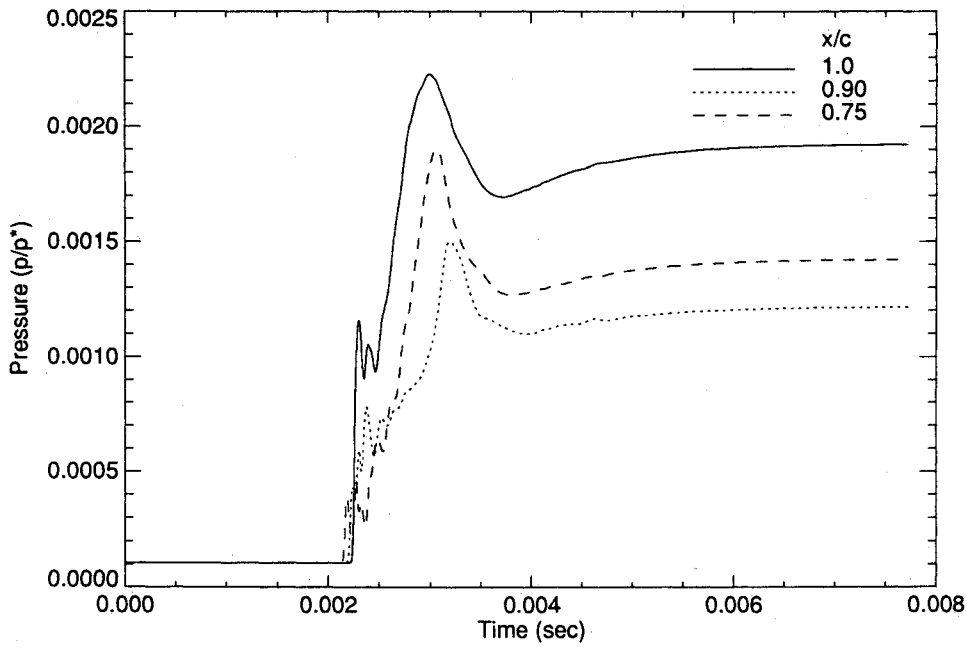

Fig. 14 Pressure distributions in the separated region of a thick double wedge.

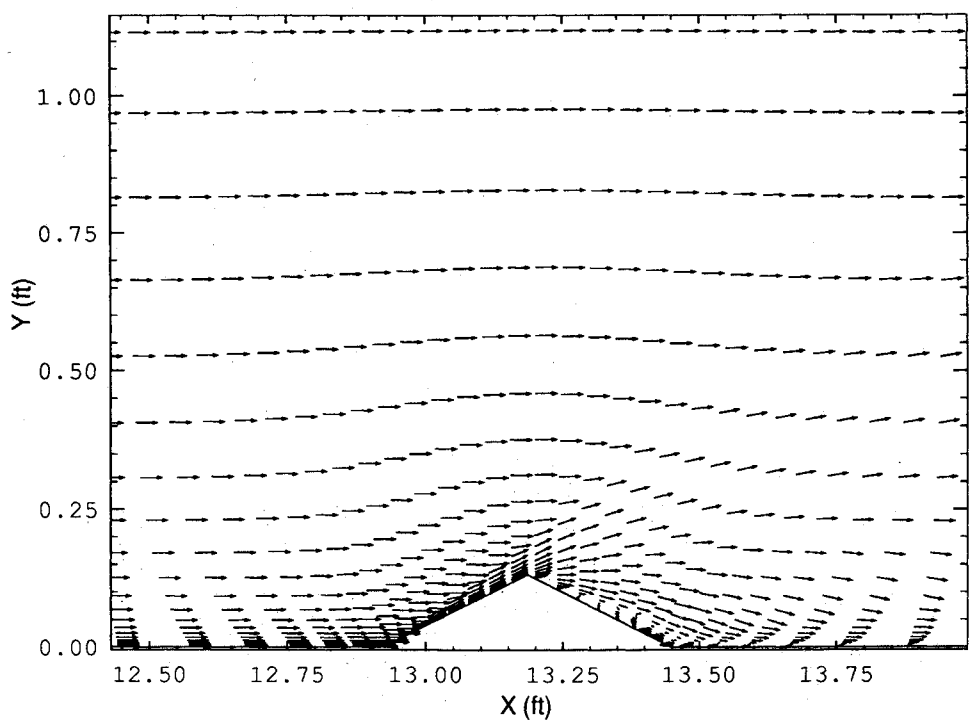

Fig. 15 Close-up of velocity vectors on a thin double wedge at $t=6.1$ ms.

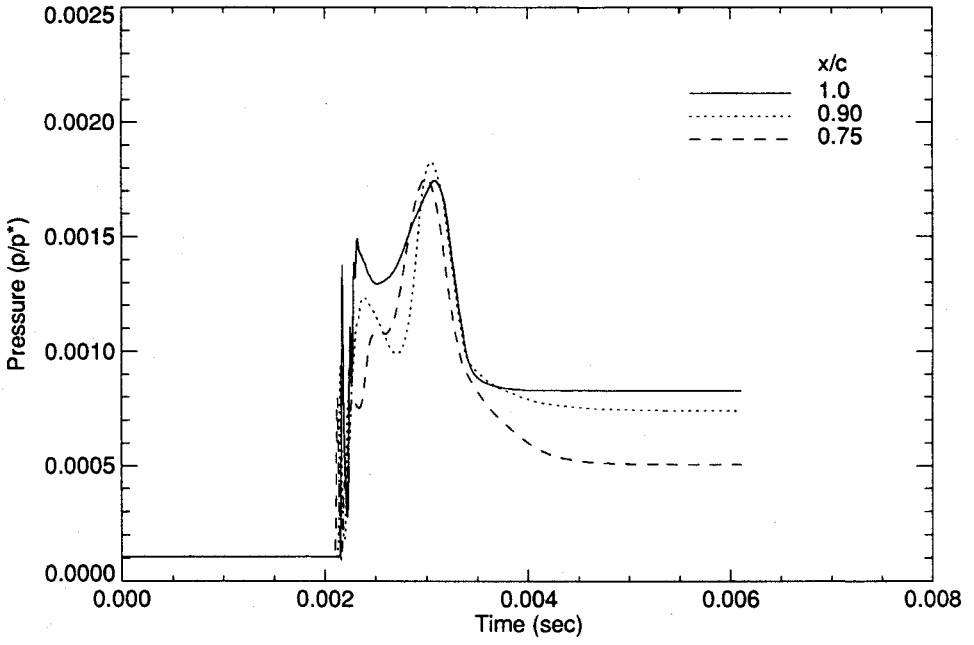

Fig. 16 Pressure distributions in the separated region of a thin double wedge.

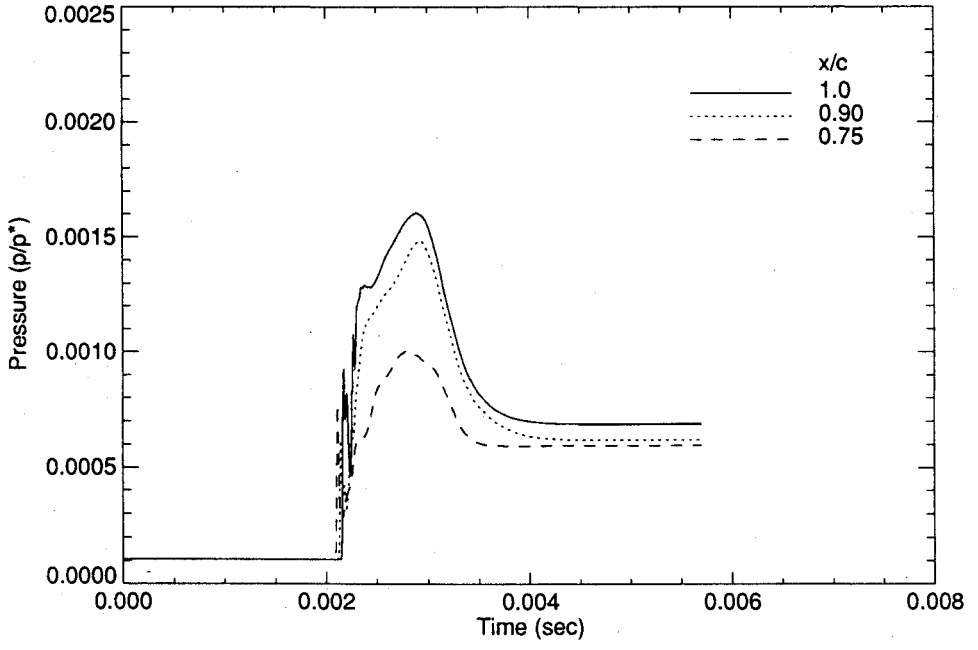

Fig. 17 Pressure distributions in the separated region of a biconvex airfoil.

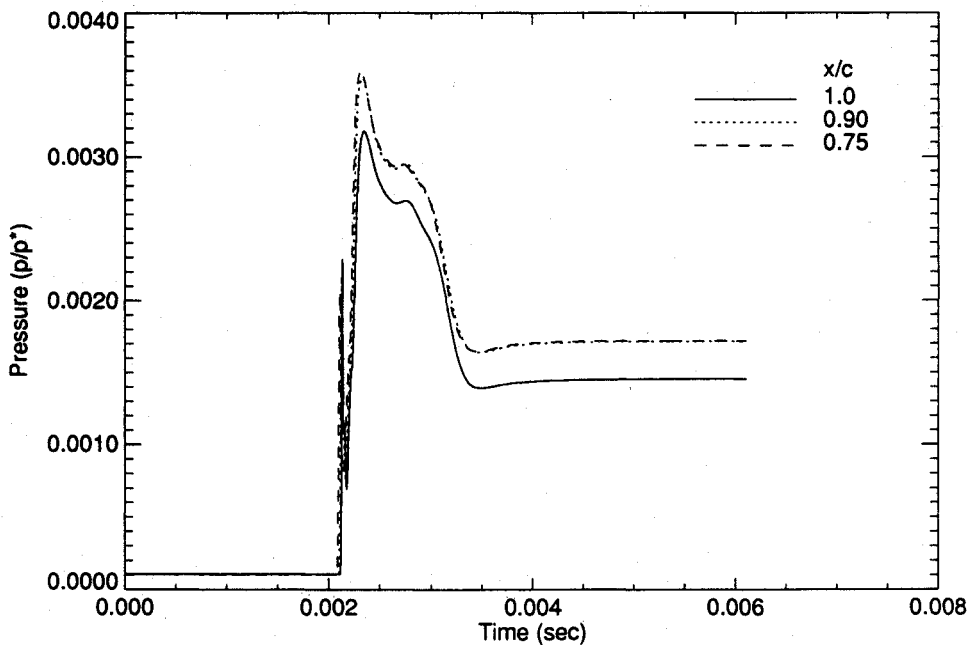

Fig. 18 Pressure distributions in the separated region of a flat plate.

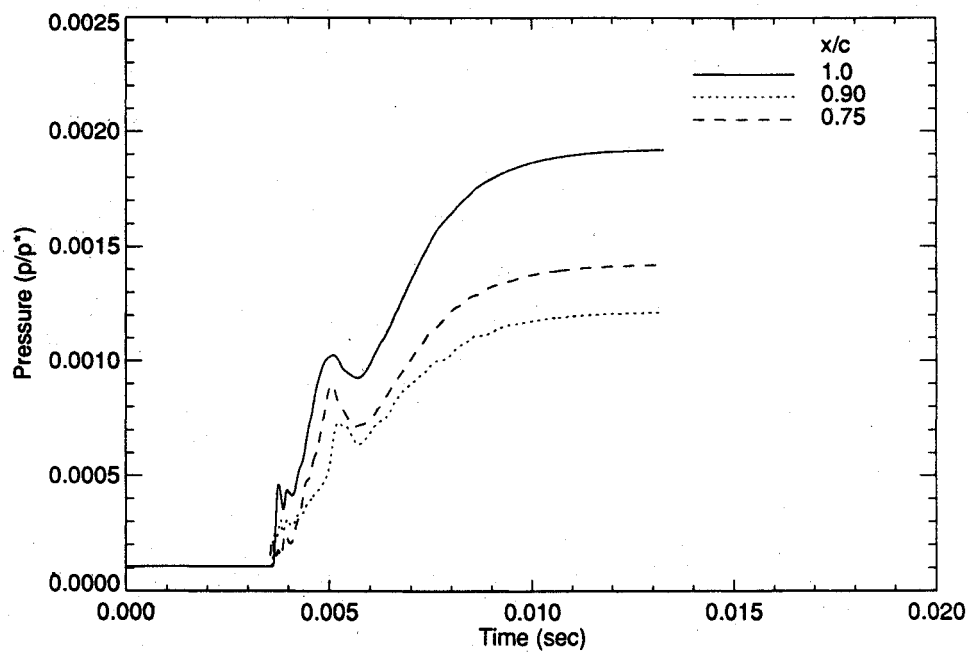

Fig. 19 Pressure distributions in the separated region of a thick double wedge at U_∞=2480 ft/s

Table 1 Flow establishment times on models U_∞=4960 ft/s

Models	τ_p, ms	$\tau_p U_\infty/L$
Flat plate	0.3	3
Biconvex airfoil	1.3	12
Thin double wedge	1.5	14
Thick double wedge	3.0	28
Circular cylinder	5.0	46

Flow over a Biconvex Airfoil

For a biconvex (t/c=0.5) airfoil, pressure records on the surface at x/c=0.9 in Fig. 17 indicate that flow reaches steady state at time t =4.3 ms. Therefore, the longest flow establishment time for pressure τ_p is determined to be 1.3 ms.

Flow over a Flat Plate

From the pressure records on the surface at x/c=1.0 in Fig. 18, it can be seen that the flow on the flat plate achieves steady state at t=3.3 ms. Therefore, the estimated flow establishment time for pressure τ_p is determined to be 0.3 ms.

Flow Establishment Times

Table 1 indicates that the calculated nondimensional flow establishment time $\tau_p U_\infty/L$ varies from 3 on a flat plate to 46 on a circular cylinder and that a flat plate has the shortest flow establishment time. The biconvex airfoil and double wedge take more time to be established, and the circular cylinder has the longest time.

To investigate the effect of changing of the freestream velocity on the flow establishment time, the flows on the models are simulated with half the freestream velocity, U_∞=2480 ft/s, which is

Table 2 Flow establishment times at different freestream velocities

Velocity, U_∞, ft/s	4960 τ_p, ms	2480 τ_p, ms
Biconvex airfoil	1.3	2.8
Thin double wedge	1.5	3.3
Thick double wedge	3.0	6.5
Circular cylinder	5.0	11.0

obtained by decreasing the stagnation temperature to T_o=766°R. Unit Reynolds number R_e at the exit is 2.1×10^8 (ft/s).

Table 2 shows the flow establishment times for various models at U_∞=2480, 4960 ft/s and verifies that the flow establishment time is inversely proportional to the freestream velocity as proposed by Holden[5] through his experiments.

Conclusion

By its very nature, this research topic requires not only the solution of the full Navier-Stokes equations but also an advanced shock-capturing numerical algorithm such as the TVD scheme because it deals with the unsteady viscous problems inside the boundary layer at hypersonic speeds. For this research, the original TIMETVD code solving the two-dimensional thin-layer Navier-Stokes equations was modified to solve the full Navier-Stokes equations.

Analyses of the results of the present study show that for a circular cylinder in a 14.7 ft long two-dimensional shock tunnel with a stagnation temperature T_o=3063°R, the unsteady viscous flow over the circular cylinder becomes stabilized within about 8 ms, which includes the starting process. The calculated nondimensional flow establishment time, $\tau_p U_\infty/D$, is 46, and it was verified that the flow establishment time increases with increasing length of the separated region and decreases with increasing freestream velocity; these results are in agreement with a correlation suggested by Holden.

Acknowledgments

A portion of this work was conducted under support of NASA Ames Research Center, with George S. Deiwert as technical monitor. The authors would like to thank H. C. Yee at NASA Ames Research Center for helpful suggestions and for providing her computer code TIMETVD as a basis for this research. Appreciation is also expressed to Chul Park at NASA Ames for valuable technical advice and James Randolph at the Mission Design Section at the Jet Propulsion Laboratory (JPL) and the people at the JPL Supercomputer Center for their generous computer time.

References

[1]Anon., "National Aero-Space Plane: A Technology Development and Demonstration Program to Build the X-30," General Accounting Office, GAO/NSIAD-88-122, N88-23764, Washington, DC, April 1988.

[2]Anderson, J. D., Jr., "A Survey of Modern Research in Hypersonic Aerodynamics," AIAA Paper 84-1578, June 1984.

[3]Lukasiewicz, J. L., *Experimental Methods of Hypersonics,* Vol. 3, Gas Dynamics Series, Marcel Dekker Publ., New York, 1973.

[4]Trimmer, L. L., Cary, A., and Voisinet, R. L., "The Optimum Hypersonic Wind Tunnel," AIAA Paper 86-0739 CP, March 1986.

[5]Holden, M. S., "Establishment Time of Laminar Separated Flows," *AIAA Journal,* Vol. 9, No. 11, 1971, pp. 2296–2298.

[6]Smith, C. E., "The Starting Process in a Hypersonic Nozzle," *Journal of Fluid Mechanics,* Vol. 24, Pt. 24, 1966, pp. 625–640.

[7]Amann, H. O., "Experimental Study of the Starting Process in a Reflection Nozzle," *The Physics of Fluids,* Supp. I, 1969, pp. 150–153.

[8]Byun, Y., Lee, J. Y., Anderson, J. D., Jr., and Kothari, A. P., "Unsteady Hypersonic Viscous Flow in Impulse Facilities," AIAA Paper 90-0421, Jan. 1990.

[9]Yee, H. C., and Harten, A., "Implicit TVD Schemes for Hyperbolic Conservation Laws in Curvilinear Coordinates," *AIAA Journal,* Vol. 25, No. 2, 1987, pp. 266–274.

[10]Yee, H. C., "A Class of High-Resolution Explicit and Implicit Shock-Capturing Methods," NASA TM 101088, Feb. 1989.

[11]Park, C., *Nonequilibrium Hypersonic Aerothermodynamics,* Wiley, New York, 1990.

[12]Roe, P. L., "Approximate Riemann Solvers, Parameter Vectors, and Difference Schemes," *Journal of Computational Physics,* Vol. 43, March 1981, pp. 357–372.

[13]Lee, J. Y., and Lewis, M. J., "A Numerical Study of the Flow Establishment Time in Hypersonic Shock Tunnel," AIAA Paper 91-1706, July 1991.

[14]Rudy, D. H., Thomas, J. L., Kumar, A., Gnoffo, P., and Chakravarthy, S. R., "A Validation Study of Four Navier-Stokes Codes for High-Speed Flows," AIAA Paper 89-1838, June 1989.

Gerald T. Chrusciel
Associate Editor